246 Multigrid Methods IV, pp. 245-256, Birkhauser Verlag 1994.

A Full Multigrid Method Applied to Turbulent Flow using the SIMPLEC Algorithm Together with a Collocated Arrangement

Peter Johansson and Lars Davidson[1]

ABSTRACT An implementation of a multigrid method in a three-dimensional SIMPLEC code based on a collocated grid arrangement is presented. The multigrid algorithm is FMG-FAS, using a V-cycle described by Brandt [1,2].
The coarse grid is obtained by merging eight fine grid cells in 3D, and four in 2D. Restriction and prolongation of field quantities are carried out by a weighted linear interpolation, and restriction of residuals by a summation. All variables and all equations, including the pressure correction equation, are treated in the same way
.
To stabilize the solution process, a fraction of the multigrid sources is included in the diagonal coefficient a_p, and a damping function is used on negative corrections of the turbulent quantities to prevent them from being negative.
The multigrid method was shown to be relative insensitive to the choice of under-relaxation parameters. Therefore 0.8 or 0.7 is used for all equations, except for the pressure correction equation where 1.5 is used.
Both turbulent and laminar calculations are presented for a 2D backward facing step, a 2D ventilated enclosure, and a 3D ventilated enclosure. The turbulent calculations are made with a two-layer low-Reynolds $k-\epsilon$ model.
Different discretization schemes for the convective schemes are used including the first order hybrid scheme and two higher order schemes (QUICK and a van Leer TVD scheme).

1 Introduction

Except for in some simple situations, calculation of flow problems is always bound to numerical methods. These numerical methods can be based on finite elements, finite volumes, finite differences, etc.

[1]Department of Thermo- and Fluid Dynamics,
Chalmers University of Technology, S-41296 Gothenburg, Sweden

Characteristic of all of these methods is that a high resolution is needed in areas of rapid changes, for example in boundary layers, shocks and recirculation regions. On the other hand, commonly used matrix solvers are dependent on grid density and often the CPU-time is quadratically dependent on the number of nodes. This conflict usually results in the accuracy of the numerical simulation being dictated by limited CPU resources rather than by considerations of the physical flow situation.

Using multigrid, the CPU-time is reduced dramatically. In fact the CPU-time is close to linearly dependent on the number of nodes, which means that higher resolution can be afforded and a more accurate solution achieved.

For incompressible flow, several laminar multigrid implementations have been presented with different variants of FAS or CS. It is much more challenging to adopt FAS to turbulent flow situations, where only a very few efforts have been reported [4,5,6]. The turbulent transport equations (such as the k and ϵ equations) increase the complexity of the equation system in many respects. The k and ϵ equations are nonlinear and source dominated. The value of the turbulent quantities (k and ϵ) must stay positive during every instant of the iteration procedure.

In the present study FAS has been employed with the SIMPLEC algorithm in 2D and 3D turbulent flow using a low-Reynolds $k-\epsilon$ model. An increased convergence rate of a factor 10-100 or even more is obtained. The turbulent multigrid calculations were shown to be stable and the number of iterations was independent of grid density, or even decreased with increasing grid density.

2 The finite volume procedure

2.1 Basic Equations

The conservation equations for incompressible turbulent flow, using the $k-\epsilon$ model, are

$$\frac{\partial}{\partial x_j}(\rho U_j \Phi) = \frac{\partial}{\partial x_j}\left(\Gamma \frac{\partial \Phi}{\partial x_j}\right) + S \tag{1}$$

where Table 1 shows the the different variables and source terms. The turbulence model used is a two-layer $k-\epsilon$ model. In the fully turbulent flow region the standard $k-\epsilon$ model is used, and near walls it is matched at a pre-selected grid line with a one-equation model. In the one-equation region the k equation is solved and the turbulent length scale is prescribed using a mixing length approach [7].

Define a flux vector J_j containing both convection and diffusion as:

$$J_j = \rho U_j \Phi - \Gamma \frac{\partial \Phi}{\partial x_j} \tag{2}$$

Integration over a control volume using Gauss law then yields:

EQUATION	Φ	Γ	S
Continuity	1	0	0
Momentum	U_i	μ_{eff}	$-\frac{\partial p}{\partial x_i}$
Turbulent kinetic energy	k	$\mu + \frac{\mu_t}{\sigma_k}$	$P_k - \rho\epsilon$
Dissipation of k	ϵ	$\mu + \frac{\mu_t}{\sigma_\epsilon}$	$\frac{\epsilon}{k}(C_{\epsilon 1} P_k - C_{\epsilon 2}\rho\epsilon)$
$P_k = \mu_t \frac{\partial U_j}{\partial x_i}\left\{\frac{\partial U_j}{\partial x_i} + \frac{\partial U_i}{\partial x_j}\right\}$		$\mu_{eff} = C_\mu \rho k^2/\epsilon + \mu$	

TABLE 1. The parameters in the general transport equation

$$\int_A n_j J_j dA = \int_V S dV \tag{3}$$

2.2 Numerical method

Representing the flux vector J_j at the cell faces and the sources in the center results in a system of matrix equations that can be written in the form:

$$a_P \Phi_P = \sum_{nb} a_{nb} \Phi_{nb} + s \tag{4}$$

The code CALC-BFC [8], where the multigrid algorithm is implemented, uses the SIMPLEC algorithm of Patankar [9], within a collocated arrangement. To aviod nonphysical oscillations, a third order pressure dissipation is introduced by Rhie and Chow interpolation [10] when the massfluxes are calculated.

The coefficients a_{nb} contain contributions due both to convection and diffusion, and the source terms contain the remaining terms. The convective part is discretized either with the Hybrid-Upwind scheme [9], the quadratic uppstream scheme QUICK [11], or a TVD scheme from van Leer [12] The diffusive part is discretized with central differencing. In SIMPLEC procedure the continuity equation is turned into an equation for a pressure correction Φ_{pp} and the solution procedure is briefly descriebed as:

1. Relax U,V,W-momentum equations
2. Calculate mass fluxes and relax the pressure correction equation.
3. Relax k and ϵ
4. Calculate the turbulent viscosity (using under-relaxation)

"Relax" means first to evaluate the coefficients and source terms in Eq. 4 and then to make a sweep with the TDMA smoother.

3 FAS applied to SIMPLEC

3.1 Description of FAS

The description below is done with two grid levels, but is easily extended to more grid levels using the V-cycle. The FAS algorithm is described here when applied to SIMPLEC. This special multigrid method originates from a laminar multigrid [13], which is similar to the concept presented by Perić *et. al.* [5]. To prepare the multigrid for local mesh refinements some changes were made before the extension to turbulent flow was performed.

For any variable on the fine grid level 2, define the residual r^2 by:

$$a_P^2 \phi_P^2 = \sum_{nb} a_{nb}^2 \phi_{nb}^2 + s^2 + r^2 \tag{5}$$

The representation at a coarse grid by FAS is then:

$$a_P^1 \phi_P^1 = \sum_{nb} a_{nb}^1 \phi_{nb}^1 + s^1 + [\overline{a}_P^1 \overline{\phi}_P^1 - \sum_{nb} \overline{a}_{nb}^1 \overline{\phi}_{nb}^1 - \overline{s}^1 - \overline{r}^1] \tag{6}$$

where $\overline{\phi}^1$ is the restricted field variable and $\overline{r}^1$ is the restricted residual obtained from the fine grid residual r^2. The source term $\overline{s}^1$ and the coefficients $\overline{a}^1$ are calculated at the coarse grid using the restricted field variables, and all overlined terms are held constant under the course of coarse grid iterations.

The overlined quantities are used as an initial guess for a^1, ϕ^1 and s^1 which are changed owing to the restricted residual $\overline{r}^1$ while iterating at the coarse grid. The changes $\delta^1 = \phi^1 - \overline{\phi}^1$ at the coarse grid are then prolongated to correct the approximation ϕ^2 obtained earlier at the fine grid.

The two-dimensional coarse grid control volume is obtained by merging four fine grid cells together, and a three-dimensional coarse grid control volume by merging eight fine grid cells together.

The residuals represent a flux imbalance according to Eq. 3. They are therefore restricted to the coarse grid by a summation of the fine grid residuals that correspond to the fine grid cells that define the coarse grid cell. Restriction and prolongation of the field quantities is made by bilinear interpolation in 2D and trilinear interpolation in 3D.

Since non-uniform grids are used, the interpolation weights are assembled locally. For the restriction these weights are simply defined by the fraction that a fine volume takes of the corresponding coarse one, while for the prolongation the weights are calculated from the distances between the centers of the fine grid volumes and the coarse volumes.

All variables $(U, V, W, P, k, \epsilon)$ are restricted and prolongated equally, and all equations are treated in the same way with just a few exceptions given in the next section.

3.2 Special features of this implementation

1. In the laminar concept [13] the mass fluxes were restricted separately in order to achieve continuity at the coarse grid. At the coarse grid, the mass fluxes were then only corrected by the changes of the velocities. In the present study the pressure correction equation is treated in the same way as the other equations, but since it is a correction equation, $\overline{\Phi_{pp}}$ is equal to zero. No special treatment of mass fluxes is now needed, which simplifies the code, especially in connection with local mesh refinement.

2. In order to prepare the present method for local mesh refinement the pressure is restricted, which produces a problem at the coarse grid with the implicit treatment of the mass fluxes. The problem is related to the Rhie and Chow interpolation, where the coefficient a_P is used to calculate the mass fluxes and the mass fluxes are needed to evaluate a_P. Therefore at a coarse grid, a_P is stored from the last V-cycle and used in the Rhie and Chow interpolation.

3. An extra sweep with the pressure correction equation and calculation of the turbulent vicosity immediately after prolongation has been shown to be efficient in preventing oscillatory behaviour.

4. To stabilize the coarse grid equations special treatment of the multigrid source term s_m

$$s_m = \overline{a}_P^1 \overline{\phi}_P^1 - \sum_{nb} \overline{a}_{nb}^1 \overline{\phi}_{nb}^1 - \overline{s}^1 - \overline{r}^1 \tag{7}$$

is used for the k and ϵ equations. If $s_m > 0$, it is included in the right hand side vector s_Φ^1, while if $s_m < 0$, is it included in the diagonal coefficient a_P^1 via a division by ϕ_P^1

5. The turbulent kinetik energy k and its dissipation ϵ cannot physically be negative. Furthermore during the iterative solution process they must stay positive. If they become negative the turbulent sources would change sign and the turbulent viscosity would be negative, which results in rapid divergence. To prevent the turbulent quantities from becoming negative after prolongation, a damping function on negative corrections, proposed by Lien [6], is used. The positive changes at a coarse grid δ_+^1 are first prolongated to give δ_+^2 and, in the same way, δ_-^2 is obtained. The turbulent quantity ϕ_*^2 at the fine grid is then corrected to ϕ^2 by $\phi^2 = \phi_*^2(\delta_+^1 + \phi_*^2)/(\phi_*^2 - \delta_-^2)$

6. The QUICK scheme can produce negative coefficents, which can destroy the diagonal dominance of the coefficient matrix. Therefore a local under-relaxation is used, as suggested by Hellström [14], so that diagonal dominace is ensured always.

3.3 Special treatment of boundary conditions

The Dirichlet conditions at the inlet at coarse grids are based on global conservation of the mass flux between the grids. Since at a boundary two cells merged together define a coarse boundary cell (in 2D), the velocity is evaluated from the sum of mass fluxes from the two fine cells.

Neumann boundary conditions are applied without any constraints at all coarse grids.

4 Applications

Three cases are presented where both laminar and turbulent calculations are performed using a two-layer $k - \epsilon$ model.

In the laminar calculations the first-order Hybrid-Upwind discretisation scheme is used. For the turbulent calculations two different combinations of discretisations are used. The first combination is as in the laminar case (Hybrid-Upwind for all equations), and the second is QUICK for the velocities together with a bounded TVD scheme of van Leer for the turbulent quantities.

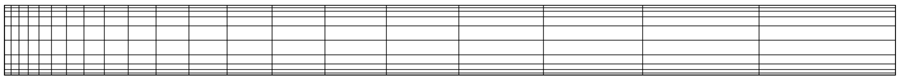

FIGURE 1. 20x10 grid for the backwards facing step

MODEL	LAMINAR		LOW-RE $k - \epsilon$			
RE	100		110 000			
SCHEME	HYBRID		HYBRID		QUICK + VAN-LEER	
	WU	SPEEDUP	WU	SPEEDUP	WU	SPEEDUP
20x10	67	1.0	185	1.0	215	1.0
40x20	58	1.9	108	3.3	130	3.1
80x40	44	6.4	72	10.8	82	∞
160x80	60	15.6	72	23.7	76	∞
320x160	91	37.5	63	100*	73	∞

TABLE 2. Convergence data for backwards facing step

The multigrid calculations were shown to be very stable, and therefore the under-relaxation parameters are set to 1.5 for the pressure correction equation and 0.7 or 0.8 for all other equations.(0.7 was used for the backwards facing step and 0.8 for the other two geometries). Decreasing the under-relaxation parameters to

0.5 decreased the convergence rate by a factor of 2 for both single grid calculations and for multigrid calculations.

Different V-cycles were tested but the convergence rate was not significantly affected and therefore a 2-1-..-1-4-1-..-1 V-cycle was used.

For each case, convergence data of the calculations are shown in tables. Convergence history plots of each geometry are also presented. Superscript * means an estimated result because the single grid is too time consuming to calculate, and ∞ means that the single grid calculation did not converge. The convergence criterion is $maxR = 0.1\%$ where $maxR$ is defined by

$$maxR = \max_{\Phi}\left[\left\{\sum_N \left| a_P\Phi_P - \sum_{nb} a_{nb}\Phi_{nb} - s \right|\right\}/F_\Phi\right] \tag{8}$$

The scaling factor F_Φ is the inlet flux for each equation.

One WU is work equivalent to one SIMPLEC sweep at the finest grid, and is comparable to the calculation of $maxR$.

4.1 2D BACKWARDS FACING STEP

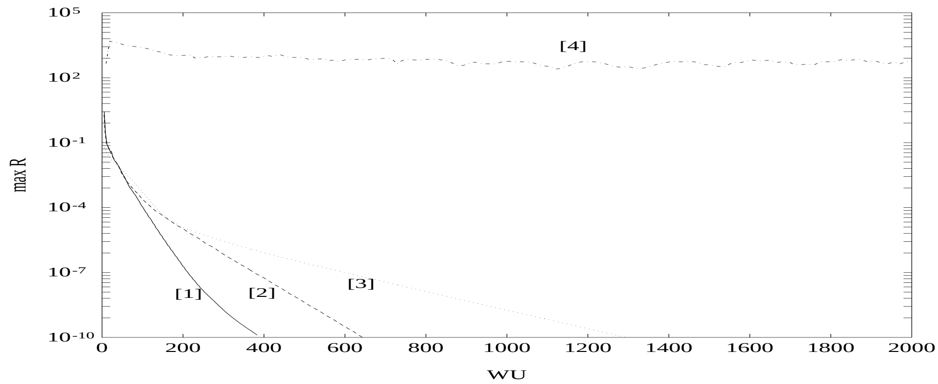

FIGURE 2. Convergence history of the 320x160 calculations for the 2D backwards facing step .[1]: Hybrid,turbulent,5-level FMG. [2]: QUICK,turbulent,5-level FMG. [3]: Hybrid,laminar,5-level FMG. [4]: Hybrid,turbulent,single grid.

The first application is a 2D backwards facing step. The inlet is half of the total height 2H. The total length of the domain is 25H, to be sure that the Neumann condition at the outlet is correct. The coarsest grid is shown in Fig. 1.

For the laminar case, a parabolic velocity profile is used at the inlet and for the turbulent case a 1/7 profile is used. The Reynolds number for the laminar calculation is 100 and 110,000 for the turbulent case.

The single grid calculations for the turbulent case were somewhat unstable at fine grids, mainly because of the high under-relaxation parameters used. To stabilize the single grid calculations, a high viscosity was used during the first ten iterations. That worked nicely for the Hybrid scheme but was insufficient with the QUICK-van Leer combination. Note that the multigrid calculations did not show these instability tendencies.

Convergence data are shown in Table 2. Notice that for the turbulent calculation the number of WU needed for convergence decreases when the mesh gets finer. The low Reynolds treatment demands high resolution near the walls, and although the mesh is expanding (see Fig. 1), 20 nodes were needed in the vertical direction. Therefore the low Reynolds area is defined from the 40x20 grid, where the first grid line is selected to be the one-equation region. A 5-level V-cycle is used for the turbulent case on a 320x160 grid, and the estimated speedup here is around 100, which is significant. Fig. 2 shows the convergence history.

4.2 2D VENTILATED ENCLOSURE

MODEL	LAMINAR		LOW-RE $k-\epsilon$			
RE	100		9000			
SCHEME	HYBRID		HYBRID		QUICK + VAN-LEER	
	WU	SPEEDUP	WU	SPEEDUP	WU	SPEEDUP
10x10	41	1.0	119	1.0	169	1.0
20x20	54	0.9	67	1.7	84	1.6
40x40	100	1.7	51	6.0	59	6.2
80x80	95	5.2	39	52.0	44	44.9
160x160	87	22.6	34	153.6	43	118.1
320x320	134	50*	30	600*	45	450*

TABLE 3. Convergence data for the 2D ventilated enclosure

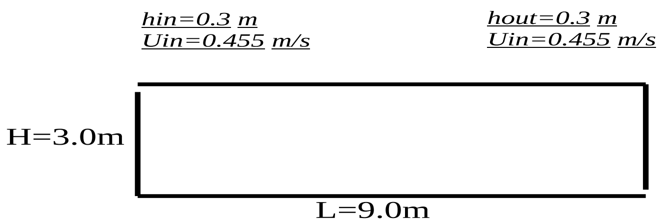

FIGURE 3. The 2D ventilated enclosure

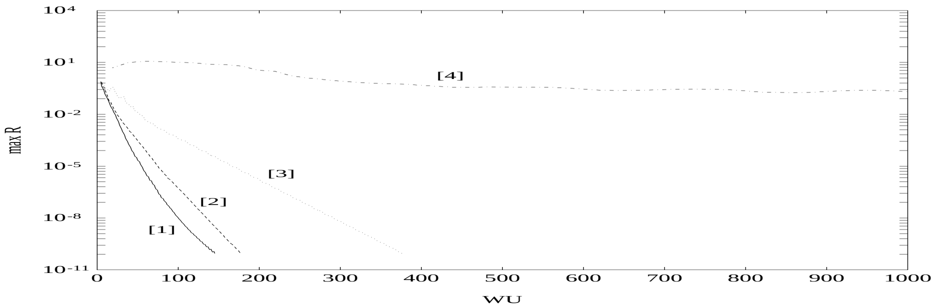

FIGURE 4. Convergence history of the 160x160 calculations for the 2D ventilated enclosure .[1]: Hybrid,turbulent,5-level FMG. [2]: QUICK,turbulent,5-level FMG. [3]: Hybrid,laminar,5-level FMG. [4]: Hybrid,turbulent,single grid.

Next configuration is a two-dimensional model of a ventilated enclosure shown in Fig. 3

The Reynolds number based on the inlet height is 100 for the laminar case and 9000 for the turbulent case. These turbulent calculations proved to be even more robust than for the backwards facing step. This is shown in Table 3 where the number of required WU decreases significantly with the grid density. Here, too, a non-uniform expanding mesh is used in order to be able to have one finite volume of the coarsest grid in the low Reynolds area.

Here the speedup is even more significant, and a 6-level V-cycle is used for the turbulent case on a 320x320 grid, wich converged 600 times faster than the estimated CPU-time of the corresponding single grid calculation. It is worth mentioning that the 320x320 FMG calculation is performed within 30 minutes on a work station (DEC 3000/400). In Figure. 4 the convergence history is shown for the 160x160 grid.

4.3 3D VENTILATED ENCLOSURE

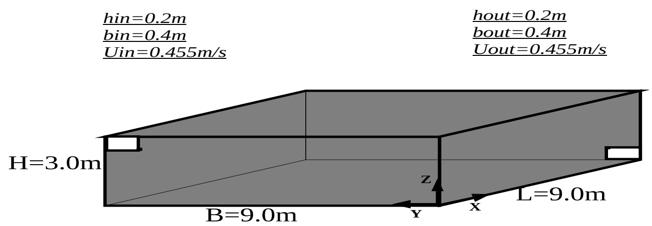

FIGURE 5. The 3D ventilated enclosure

The configuration of the three-dimensional ventilated enclosure is shown in Fig. 5

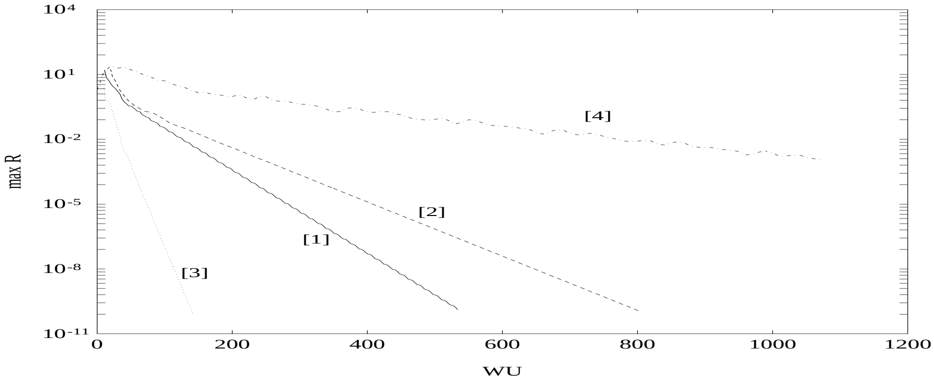

FIGURE 6. Convergence history of the 40x40x40 calculations for the 3D ventilated enclosure. [1]: Hybrid,turbulent,4-level FMG. [2]: QUICK,turbulent,4-level FMG. [3]: Hybrid,laminar,4-level FMG. [4]: Hybrid, turbulent single grid

The Reynolds number based on the inlet hydraulic diameter is 100 for the laminar case and 8200 for the turbulent case. The turbulent flow becomes very complex inside the enclosure, which is shown in Fig. 7.

This complexity also affects the convergence rate, where a typical number of required WU is around 200 while for the other two cases only around 50 were needed. Table 3 shows, however, that the number of required WU is constant or decreasing for increasing grid density, except for the finest laminar cube. Here, too, a non-uniform expanding mesh is used to be able to have one finite volume in the low Reynolds area at the coarsest mesh.

The speedup for this configuration is not very significant since the grid density is not very high. Nevertheless, a speedup factor of 20 at a 4-level V-cycle with the $k - \epsilon$ model on a 80x80x80 grid is considerable. Fig. 6 shows the convergence history for the 40x40x40 grid.

It is interesting to note that when injection was used instead of this prolongation, on the QUICK-van Leer combination, the only effect was that the convergence rate was slowed down by a factor 2. If the weights were set as if the mesh was uniform, the convergence rate was not significantly affected either. On non-orthogonal meshes, where the evaluation of the local weights is too time consuming, the convergence would therefore probably not be much affected much if fixed weights were used.

5 Closure

Some indications from the present investigation are worth pointing out:
1. Multigrid accelleration is highly effective in 2D and 3D laminar and turbulent

MODEL	LAMINAR		LOW-RE $k - \epsilon$			
RE	100		8200			
SCHEME	HYBRID		HYBRID		QUICK + VAN-LEER	
	WU	SPEEDUP	WU	SPEEDUP	WU	SPEEDUP
10x10x10	52	1.0	213	1.0	478	1.0
20x20x20	45	2.8	215	2.0	332	∞
40x40x40	49	9.0	170	4.8	221	∞
80x80x80	116	20*	218	20*	-	-

TABLE 4. Convergence data for 3D ventilated enclosure

flows, with observed speedup factors larger than 100.
2. The CPU-time of the multigrid calculations is linearly dependent of the number of nodes for both laminar and turbulent flows.
3. The effectivness is not greatly affected of grid non-uniformity.
4. Neumann boundary conditions can be handled as well as Dirchlet conditions.

6 References

[1] A. Brandt, Multi-level adaptive solutions to boundary-value problems. *Math. of Comput.*, Vol.31 333-390 (1977)
[2] A. Brandt, *Multigrid techniques: 1984 guide with applications to fluid dynamics.* Computational fluid dynamics lecture notes at von-Karman Institute, (1984)
[3] G. J. Shaw and S. Sivaloganathan, On the smoothing properties of the SIMPLE pressure-correction algorithm, *Int. J. Num. Meth. Fluids*,Vol. 8, 441-461 (1988)
[4] Y. Li, L. Fuchs S. Holmberg, An evaluation of a computer code for predicting indoor airflow and heat transfer., *12th AIVC Conf.* , Ottawa Canada (1991)
[5] M. Perić, M. Rüger and G. Scheuerer, A finite volume multigrid method for calculating turbulent flows., *Proc. 7th Symp. on Turb. Shear Flows*,7.3.1-7.3.6 Stanford, (1989)
[6] F.S. Lien, M.A. Leschziner, Multigrid convergence accelleretion for complex flow including turbulence., *Multigrid methods III* Birkhäuser Verlag. (1991)
[7] H.C. Chen V.C. Patel, Practical near-wall turbulence models for complex flows including separation., *AIAA paper 87-1300*, Honolulu (1987)
[8] L. Davidson, B. Farhanieh, A finite volume code employing colocated vari-

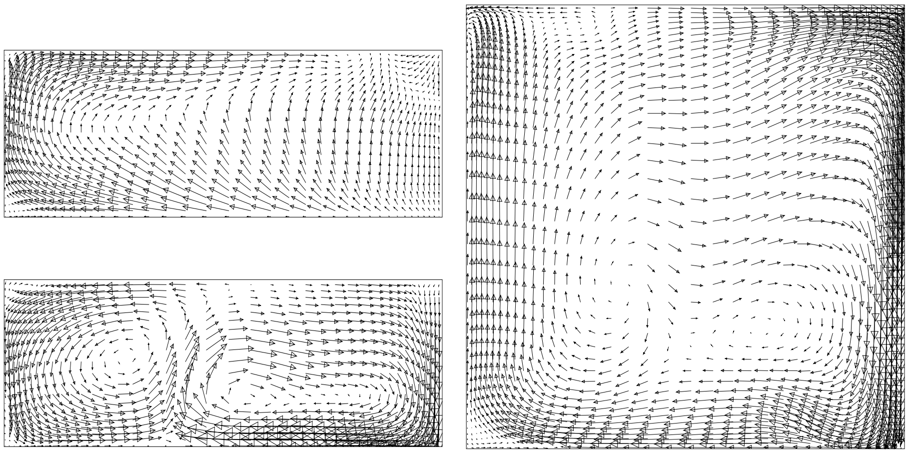

FIGURE 7. Vector plots at x/L=0.5 (upper left), y/B=0.5 (lower left) and z/H=0.5 for the three-dimensional ventilated room

able arrangement and cartesian velocity components of fluid flow and heat transfer in complex three-dimensional geometries. Rept. 91/14 Dep. of Thermo- and Fluid Dyn.,Chalmers Univ. of Techn. (1991)

[9] S.V. PATANKAR, *Numerical heat transfer and fluid flow*, Hemispere Publishing Co., McGraw Hill, (1980)

[10] C.M RHIE, W.L. CHOW, Numerical study of the turbulent flow past an airfoil with trailing edge separation., *AIAA J.* Vol. 21, 1525-1532 (1983)

[11] B.P. LEONARD, A stable and accurate convective modelling procedure based on quadratic upstream interpolation *Comput. Meth. in Appl. Mech and Eng.* Vol. 19, 59-98 (1979)

[12] B. VAN LEER, Towards the ultimate conservation difference scheme. II. Monotonocity and conservation combined in a second-order scheme *J. of Comput. Phys.* Vol. 14, 361-370 1974

[13] P. JOHANSSON, A three-dimensional laminar multigrid method applied to the SIMLEC algorithm, Diploma Thesis, Rept. 92/5 Dep. of Thermo- and Fluid Dyn.,Chalmers Univ. of Techn. (1992)

[14] T. HELLSTRÖM, DAVIDSON L., A multiblock-moving mesh extension to the CALC-BFC code. Rept. 93/3 Dep. of Thermo- and Fluid Dyn.,Chalmers Univ. of Techn. (1993)